Theoretical investigation of the behavior of titratable groups in proteins†

Astrid R. Klingen,[a] Elisa Bombarda[a,b] and G. Matthias Ullmann*[a]

Received 31st October 2005, Accepted 15th March 2006
First published as an Advance Article on the web 12th April 2006
DOI: 10.1039/b515479k

This paper presents a theoretical analysis of the titration behavior of strongly interacting titratable residues in proteins. Strongly interacting titratable residues exist in many proteins such as for instance bacteriorhodopsin, cytochrome *c* oxidase, cytochrome bc_1, or the photosynthetic reaction center. Strong interaction between titratable groups can lead to irregular titration behavior. We analyze under which circumstances titration curves can become irregular. We demonstrate that conformational flexibility alone can not lead to irregular titration behavior. Strong interaction between titratable groups is a necessary, but not sufficient condition for irregular titration curves. In addition, the two interacting groups also need to titrate in the same pH-range. These two conditions together lead to irregular titration curves. The mutation of a single residue within a cluster of interacting titratable residues can influence the titration behavior of the other titratable residues in the cluster. We demonstrate this effect on a cluster of four interacting residues. This example underlines that mutational studies directed at identifying the role of a certain titratable residue in a cluster of interacting residues should always be accompanied by an analysis of the effect of the mutation on the titration behavior of the other residues.

Introduction

The function of biomolecules is often governed by their electrostatics. Charged protein residues are for instance involved in ligand binding, enzymatic catalysis and proton pumping activity. Since several of the naturally occurring amino acid sidechains can undergo reversible protonation reactions, the charge distribution in a protein depends on pH. The titration behavior of individual residues is often complicated by the interaction between titratable residues in a protein. Strong electrostatic interactions between titratable residues has been demonstrated for many proteins.[1–16] Such strong interactions can lead to irregular titration curves. In order to understand how the electrostatics of a protein steers its function, one needs to understand the behavior of its titratable residues.

Several experimental methods such as nuclear magnetic resonance (NMR) spectroscopy, Fourier-transform infrared (FTIR) spectroscopy or calorimetric methods have been applied to analyze the titration behavior of proteins. While thermodynamic methods such as calorimetry measure macroscopic properties of a system, methods such as NMR or FTIR observe properties of individual residues in the protein. The relation between these two distinctly different types of titration experiments has been discussed in previous publications.[17–19]

Often, the behavior of titratable residues in proteins is investigated by mutational studies. Although the mutational approach is commonly used, the analysis of the results is not straight-forward and the experiments are often not conclusive. The mutation of a residue within a cluster of interacting titratable sites is likely to alter the behavior of other titratable residues in a way that is difficult to predict. If titratable residues interact strongly, a simple interpretation of the change of the titration behavior, *e.g.* the assignment of a pK_a value to an individual titratable residue, is often not possible. The standard reaction free energy for protonating a group in aqueous solution is given by $G_a^o = -RT \ln 10\ pK_a$, where R is the universal gas constant and T the temperature.

The effect of the protein environment on the protonation energy compared to the effect of the aqueous solution can be divided into three contributions: the difference in solvation energy, the interaction with non-titratable charges and dipoles of the protein, and the interaction with other titratable groups.[20–23] While the change in solvation energy and the interaction with permanent charges of the protein can shift the titration curve of a titratable residue, they cannot lead to irregular titration behavior. In contrast, the interaction between different titratable groups can result in highly irregular and even non-monotonic titration curves.[17,24,25]

We have recently demonstrated[17] that the total titration curve of any polyprotic acid with N titratable sites can be described as a sum of N non-interacting sites, so-called quasi-sites. The titration curves of the real individual sites are a linear combination of the titration curves of these quasi-sites. In contrast to the inflection or half-protonation points of the real individual titration curves, the quasi-site pK_a values are thermodynamically precisely defined pK_a values. The formalism to describe the relationship between real sites and quasi-sites is called decoupled sites representation (DSR). It is a useful tool to understand the often complicated titration behavior of interacting titratable groups in proteins.

This paper has two major goals: first, to demonstrate, based on concrete examples, when and why titration curves of individual sites in proteins become irregular, and second, to analyze how mutations within clusters of interacting titratable residues

[a]*Structural Biology / Bioinformatics, University of Bayreuth, Universitätsstr. 30, BGI, D-95447 Bayreuth, Germany. E-mail: Matthias.Ullmann@uni-bayreuth.de; Fax: +49-921-55-3544*
[b]*Département Pharmacochimie de la Communication Cellulaire-UMR 7175-LC1, Université Louis Pasteur, 74, route du Rhin, F-67401, Illkirch Cedex, France*

† This paper was published as part of the special issue on Proton Transfer in Biological Systems.

 This journal is © The Royal Society of Chemistry and Owner Societies 2006

influence their titration behavior. In the Theory section, we will give a short outline of the theory of multiple sites titration. Based on the examples of a single residue in two conformations, and two interacting titratable residues in one conformation, we will then analyze when and why titration curves become irregular. The effect of mutations is studied based on a cluster of four interacting titratable groups. This example demonstrates that mutations of residues in clusters of interacting groups can lead to changes in the titration behavior of other residues in the cluster.

Theory

Single site titration

The protonation equilibrium of a monoprotic acid can be described by

$$\mathrm{HA} \underset{}{\overset{K_a}{\rightleftharpoons}} \mathrm{A^-} + \mathrm{H^+}; \qquad K_a = \frac{[\mathrm{A^-}][\mathrm{H^+}]}{[\mathrm{HA}]}, \tag{1}$$

where K_a is the equilibrium constant and [A$^-$], [HA] and [H$^+$] represent the concentrations of the deprotonated species, the protonated species, and the protons, respectively. The pH of the solution and the pK_a value of an acid are defined as the negative decimal logarithm of the proton concentration (pH $= -\lg[\mathrm{H^+}]$) and the K_a value (p$K_a = -\lg K_a$), respectively. Using these definitions, one obtains the Henderson–Hasselbalch equation from eqn (1). The protonation probability $\langle x \rangle$ of a titratable group is given by eqn (2), which is algebraically equivalent to the Henderson–Hasselbalch equation:

$$\langle x \rangle = \frac{10^{\mathrm{p}K_a - \mathrm{pH}}}{1 + 10^{\mathrm{p}K_a - \mathrm{pH}}}. \tag{2}$$

This equation describes the standard sigmoidal titration curve that is commonly found in textbooks. The denominator of eqn (2) corresponds to the partition function of the system.

By rearranging eqn (2), it is possible to calculate the pK_a value from the protonation probability. The pK_a value is defined from the law of mass action in eqn (1) and has a clear relation to the standard reaction free energy G_a° for protonating a titratable group. The energy for protonating a group at a certain pH is given by $G_a = G_a^\circ - \mu_{\mathrm{H^+}} = -RT \ln 10\,(\mathrm{p}K_a - \mathrm{pH})$, where $\mu_{\mathrm{H^+}}$ is the chemical potential of the protons in solution.

Basic theory of multiple sites titration

A protein that has N proton binding sites and can exist in M conformations can adopt $2^N M$ different microstates. Each microstate is characterized by a vector $\boldsymbol{x}$ which specifies the protonation state ($x_i = 1$ if group i is protonated, 0 if it is deprotonated), and a number m which specifies the conformation. The partition function of such a protein in terms of microstate standard free energies $G^\circ_{\boldsymbol{x},m}$ is then given by

$$Z = \sum_m^M \sum_{\boldsymbol{x}}^{2^N} \mathrm{e}^{-\beta G^\circ_{\boldsymbol{x},m}}\, \mathrm{e}^{\beta n_{\boldsymbol{x}} \mu_{\mathrm{H^+}}}, \tag{3}$$

where $n_{\boldsymbol{x}} = \sum_{i=1}^{N} x_i$ is the number of protons bound to the molecule in state $\boldsymbol{x}$, and $\beta = 1/RT$. The partition function is a polynomial of the variable $\mathrm{e}^{\beta\mu_{\mathrm{H^+}}}$, and eqn (3) is therefore also referred to as binding polynomial.[26] The sum of the Boltzmann factors $\mathrm{e}^{-\beta G^\circ_{\boldsymbol{x},m}}$ of the states $\boldsymbol{x}$ each having $n_{\boldsymbol{x}}$ protons bound in all M possible conformations give the $n_{\boldsymbol{x}}$th coefficient of the polynomial:

$$Z = \sum_m^M \sum_{\boldsymbol{x}}^{2^N} \delta(1)\, \mathrm{e}^{-\beta G^\circ_{\boldsymbol{x},m}}\, \mathrm{e}^{\beta\mu_{\mathrm{H^+}}} + \sum_m^M \sum_{\boldsymbol{x}}^{2^N} \delta(2)\, \mathrm{e}^{-\beta G^\circ_{\boldsymbol{x},m}}\, \mathrm{e}^{\beta 2\mu_{\mathrm{H^+}}} + \cdots + \sum_m^M \sum_{\boldsymbol{x}}^{2^N} \delta(N)\, \mathrm{e}^{-\beta G^\circ_{\boldsymbol{x},m}}\, \mathrm{e}^{\beta N\mu_{\mathrm{H^+}}} \tag{4}$$

with $\delta(k) = 1$ if the state $\{\boldsymbol{x},m\}$ has k protons bound and otherwise 0. The probability that a particular site i is protonated in the molecule, *i.e.* the titration curve of an individual site is given by

$$\langle x_i \rangle = \frac{1}{Z} \sum_m^M \sum_{\boldsymbol{x}}^{2^N} x_i\, \mathrm{e}^{-\beta G^\circ_{\boldsymbol{x},m}}\, \mathrm{e}^{\beta n_{\boldsymbol{x}} \mu_{\mathrm{H^+}}} \tag{5}$$

One can assign microscopic equilibrium constants to all equilibria between different microstates of the protein. These microscopic equilibrium constants can be defined in analogy to the equilibrium constant of a monoprotic acid (see eqn (1)). For example, a simple system with only two titratable sites has the following microstates (see Fig. 1(a)): both sites protonated (11), only the first site deprotonated (01), only the second site deprotonated (10), and both sites deprotonated (00). The following microscopic equilibrium constants K_r^p where the $\boldsymbol{r}$ denotes the reactant protonation state vector and $\boldsymbol{p}$ the product protonation state vector, can thus be defined:

$$K_{11}^{01} = \frac{[(01)][\mathrm{H^+}]}{[(11)]}; \quad K_{11}^{10} = \frac{[(10)][\mathrm{H^+}]}{[(11)]};$$
$$K_{01}^{00} = \frac{[(00)][\mathrm{H^+}]}{[(01)]}; \quad K_{10}^{00} = \frac{[(00)][\mathrm{H^+}]}{[(10)]}. \tag{6}$$

The microscopic pK_r^p values are defined as the negative decimal logarithm of the microscopic equilibrium constants K_r^p (p$K_r^p = -\lg K_r^p$). They are connected to the free energy difference of the relevant microstates at standard conditions as

$$\mathrm{p}K_r^p = \frac{1}{RT \ln 10}(G_p^\circ - G_r^\circ) \tag{7}$$

The macroscopic p$\bar{K}_k$ values characterize the equilibria between two macroscopic protonation states of the protein, *i.e.* between two macrostates with k and $k-1$ protons bound. The kth macroscopic p$\bar{K}_k$ value is given by

$$\mathrm{p}\overline{K_k} = -\lg \left(\frac{\sum_m^M \sum_{\boldsymbol{x}}^{2^N} \delta(k-1)\, \mathrm{e}^{-\beta G^\circ_{\boldsymbol{x},m}}}{\sum_m^M \sum_{\boldsymbol{x}}^{2^N} \delta(k)\, \mathrm{e}^{-\beta G^\circ_{\boldsymbol{x},m}}} \right). \tag{8}$$

A macroscopic p$\bar{K}_k$ value is a thermodynamic average over all microscopic equilibria involved in the release of the kth proton. The product over the first to the kth macroscopic $\bar{K}_k$ values equals the kth polynomial coefficient $\sum_m^M \sum_{\boldsymbol{x}}^{2^N} \delta(k)\, \mathrm{e}^{-\beta G^\circ_{\boldsymbol{x},m}}$ of the partition function in eqn (4). The macroscopic p$\bar{K}_k$ values can consequently also be used to formulate the partition function. Moreover, the total titration curve of a polyprotic acid is often interpreted in terms of macroscopic p$\bar{K}_k$ values.

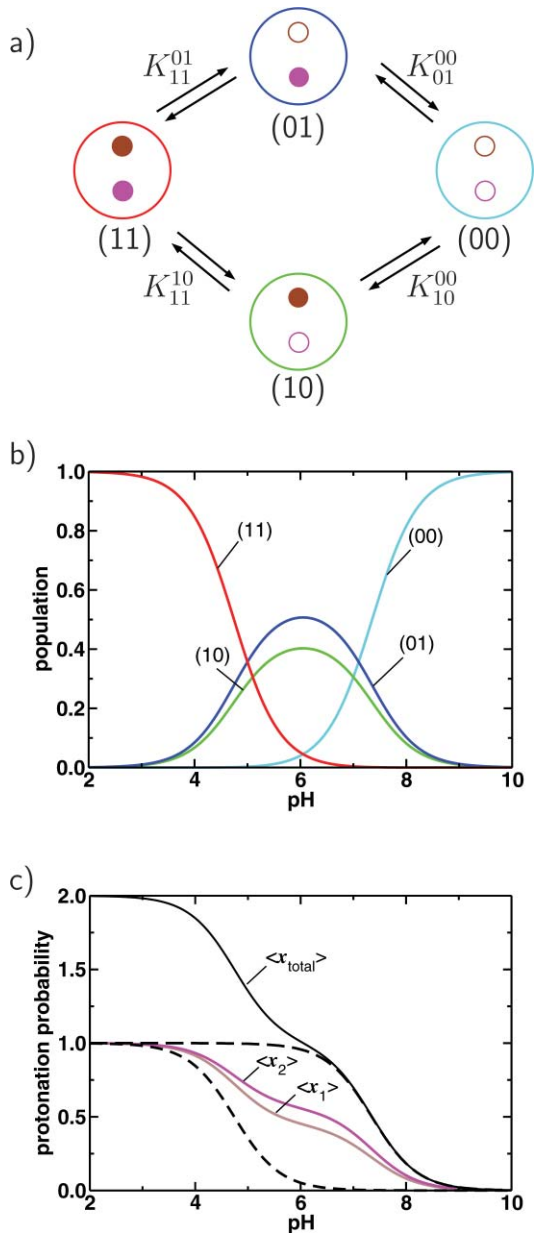

Fig. 1 Titration behavior of a diprotic acid with an interaction energy $W = 2.0$ pK units between the two sites, and microscopic pK values $pK_{10}^{00} = 7.0$ and $pK_{01}^{00} = 7.1$. (a) The four different protonation states of the system and their interconversion. Filled circles represent a protonated site, open circles a deprotonated site. The corresponding protonation state vectors are given below the states. (b) Probability to find the system in either one of the four different microstates. Color-coding of the different microstates corresponds to panel (a), the curves are marked by the corresponding protonation state vector. (c) Titration behavior of the system. The protonation probabilities of the two real sites are shown in colors corresponding to (a). The black solid line is the overall titration curve, the dashed lines show the protonation probabilities of the two independent quasi-sites of the decoupled sites representation.

Decoupled sites representation

In the framework of the DSR, the titration behavior of a protein is described in terms of decoupled quasi-sites.[17,26–29] The pK'_j values of these quasi-sites are obtained as negative decimal logarithm of the negative of the roots of the partition function in eqn (3). The titration curves of every individual real site $\langle x_i \rangle$ in a polyprotic acid with N proton binding sites can be expressed as a linear combination of the titration curves $\langle y_j \rangle$ of N decoupled quasi-sites:[17]

$$\begin{pmatrix} \langle x_1 \rangle \\ \langle x_2 \rangle \\ \vdots \\ \langle x_N \rangle \end{pmatrix} = \begin{pmatrix} a_{11} & a_{12} & \cdots & a_{1N} \\ a_{21} & a_{22} & \cdots & a_{2N} \\ \vdots & \vdots & \cdots & \vdots \\ a_{N1} & a_{N2} & \cdots & a_{NN} \end{pmatrix} \begin{pmatrix} \langle y_1 \rangle \\ \langle y_2 \rangle \\ \vdots \\ \langle y_N \rangle \end{pmatrix}, \tag{9}$$

or more simply

$$\langle x_i \rangle = \sum_j^N a_{ij} \langle y_j \rangle. \tag{10}$$

Each of the quasi-site titration curves $\langle y_j \rangle$ has a sigmoidal shape as given by eqn (2). Since each real and also each quasi-site can only bind one proton, the sum over all rows and also the sum over all columns in the a_{ij}-matrix must equal one:[17]

$$\sum_i^N a_{ij} = \sum_j^N a_{ij} = 1. \tag{11}$$

Here we give a short version of the derivation of the DSR, with an extension to multiple conformations per protonation state. Analogously to real microstates, one can define quasi-state vectors $\boldsymbol{y}$ where y_j is 1 or 0 depending if quasi-site j is protonated or not. The standard free energy of a micro-quasi-state G_y° in terms of quasi-site pK'_j values is given by

$$G_y^\circ = -RT \ln 10 \sum_j^N y_j \, pK'_j. \tag{12}$$

The protonation probability of a quasi-site is

$$\langle y_j \rangle = \frac{1}{Z} \sum_y^{2^N} y_j \, e^{-\beta G_y^\circ} \, e^{\beta n_y \mu_{H^+}}. \tag{13}$$

The matrix of the coefficients a_{ij} is obtained from the solution of N systems of linear equations, each of them having N dimensions.[17] The systems of equations are of the type

$$\boldsymbol{c}_i = \boldsymbol{B}\boldsymbol{a}_i, \tag{14}$$

with

$$\boldsymbol{c}_i = \frac{1}{\sum_m^M \sum_x^{2^N} \delta(0) \, e^{-\beta G_{x,m}^\circ}} \begin{pmatrix} \sum_m^M \sum_x^{2^N} x_i \delta(1) e^{-\beta G_{x,m}^\circ} \\ \sum_m^M \sum_x^{2^N} x_i \delta(2) e^{-\beta G_{x,m}^\circ} \\ \vdots \\ \sum_m^M \sum_x^{2^N} x_i \delta(N) e^{-\beta G_{x,m}^\circ} \end{pmatrix}, \tag{14a}$$

$$\boldsymbol{B} = \begin{pmatrix} \sum_y^{2^N} y_1 \delta(1) e^{-\beta G_y^\circ} & \sum_y^{2^N} y_2 \delta(1) e^{-\beta G_y^\circ} & \cdots & \sum_y^{2^N} y_N \delta(1) e^{-\beta G_y^\circ} \\ \sum_y^{2^N} y_1 \delta(2) e^{-\beta G_y^\circ} & \sum_y^{2^N} y_2 \delta(2) e^{-\beta G_y^\circ} & \cdots & \sum_y^{2^N} y_N \delta(2) e^{-\beta G_y^\circ} \\ \vdots & \vdots & \cdots & \vdots \\ \sum_y^{2^N} y_1 \delta(N) e^{-\beta G_y^\circ} & \sum_y^{2^N} y_2 \delta(N) e^{-\beta G_y^\circ} & \cdots & \sum_y^{2^N} y_N \delta(N) e^{-\beta G_y^\circ} \end{pmatrix}, \tag{14b}$$

 This journal is © The Royal Society of Chemistry and Owner Societies 2006

$$\boldsymbol{a}_i = \begin{pmatrix} a_{i1} \\ a_{i2} \\ \vdots \\ a_{iN} \end{pmatrix} \tag{14c}$$

The factors $x_i\delta(n)$ and $y_j\delta(n)$ filter out the states that have n protons bound and are respectively protonated at the real site i or at the quasi-site j.

The description of individual titration curves $\langle x_i \rangle$ of a molecule in terms of quasi-sites is as general as the description of eqn (5). The a_{ij}-matrix indicates how much the jth quasi-site $\mathrm{p}K'_j$ value contributes to the total protonation of the ith real site.

Calculation of microstate energies

In this paper, we use a formulation for the energy of a given microstate of a protein that is composed of three contributions: first, the energy to protonate a certain group while all other titratable groups in the protein are in their uncharged protonation form (reference form), second, the interaction energy between the titratable groups, and third, an energy attributed to the respective conformation. The standard free energy of a microstate $\{\boldsymbol{x},m\}$ is accordingly written as

$$G^{\circ}_{\boldsymbol{x},m} = -\sum_{i}^{N} \left((x_i^m - x_i^0) RT \ln 10\, \mathrm{p}K^m_{\mathrm{intr},i} \right) + \frac{1}{2} \sum_{i}^{N} \sum_{j}^{N} \left(W^m_{ij} (x_i^m - x_i^0)(x_j^m - x_j^0) \right) + G^m_{\mathrm{conf}}. \tag{15}$$

$\mathrm{p}K^m_{\mathrm{intr},i}$ is the intrinsic pK value of site i, *i.e.* the pK value that site i would have if all other titratable sites were in their reference protonation form. W^m_{ij} is the interaction between the charged forms of sites i and j. The vector $\boldsymbol{x}^0 = (x_1^0,\ldots,x_N^0)$ defines the reference protonation state. G^m_{conf} is the energy of conformation m in the reference protonation state. While we use this specific formulation for the microstate energy, it should however be stressed that the DSR formalism does not depend on the formulation of the energy function.

Computation of the DSR parameters

The DSR parameters are obtained with our program DeSiRe. Eqn (15) provides a feasible way to calculate the energy of each microstate, since the energy parameters $\mathrm{p}K^m_{\mathrm{intr},i}$ and W^m_{ij} can be computed by solving the linearized Poisson–Boltzmann equation.[30,31] The coefficients in the binding polynomial of eqn (3) can be obtained from the microstate energies. Then, the roots of eqn (3) are computed numerically using an eigenvalue method.[32] The coefficient matrix $\boldsymbol{B}$ on the right hand side of eqn (14) is derived from these roots of eqn (3) using eqn (12). The vectors $\boldsymbol{c}_i$ on the left hand side of eqn (14) are calculated from the intrinsic $\mathrm{p}K^m_{\mathrm{intr},i}$ values and interaction energies W^m_{ij} using eqn (15). Standard numerical methods (lower and upper triangular decomposition[32]) are used to solve the system of linear equations in eqn (14).

Results and discussion

The origin of irregular titration curves

The behavior of titratable residues in biomolecules is influenced by many different factors, such as conformational flexibility and interaction among different titratable groups. Using concrete examples, we demonstrate which factors can lead to irregular, non-sigmoidal titration behavior.

Conformational variability does not lead to non-sigmoidal titration curves. We have studied the titration behavior of a molecule with a single titratable group that exists in two different conformations. In the formulation of the partition function for this system, microstate energies are expressed relative to the energy of a reference microstate. Relative microstate energies are sufficient to calculate any probability quantity. The deprotonated form of the group in conformation 1 is chosen as the reference microstate. The partition function of the model system can then be written as

$$Z = 1 + \mathrm{e}^{-\beta\Delta G_{\mathrm{conf}}} + \mathrm{e}^{-\beta(\mathrm{pH}-\mathrm{p}K_{\mathrm{a},1})} + \mathrm{e}^{-\beta(\Delta G_{\mathrm{conf}} + (\mathrm{pH}-\mathrm{p}K_{\mathrm{a},1} - \Delta\mathrm{p}K_{\mathrm{a}}))}, \tag{16}$$

where $\Delta G_{\mathrm{conf}} = G_{\mathrm{conf},2} - G_{\mathrm{conf},1}$ is the energy difference (in pK units) between the two conformations in the deprotonated form, β is the inverse of RT in pK units. The pK value of the molecule in conformation 1 is $\mathrm{p}K_{\mathrm{a},1}$, and $\Delta\mathrm{p}K_{\mathrm{a}} = \mathrm{p}K_{\mathrm{a},1} - \mathrm{p}K_{\mathrm{a},2}$ is the pK_{a} difference between the two conformations. The four summands are derived from the relative energies of the four different microstates of the system: (conformation 1, deprotonated); (conformation 2, deprotonated); (conformation 1, protonated); (conformation 2, protonated).

The titration behavior of a model system is shown in Fig. 2 with the setting of the different parameters given as the figure legend. According to eqn (8), the pK value of the system can be calculated as

$$\mathrm{p}\overline{K} = -\lg \frac{1 + \mathrm{e}^{-\beta\Delta G_{\mathrm{conf}}}}{\mathrm{e}^{-\beta(-\mathrm{p}K_{\mathrm{a},1})} + \mathrm{e}^{-\beta(\Delta G_{\mathrm{conf}} - \mathrm{p}K_{\mathrm{a},1} - \Delta\mathrm{p}K_{\mathrm{a}})}}. \tag{17}$$

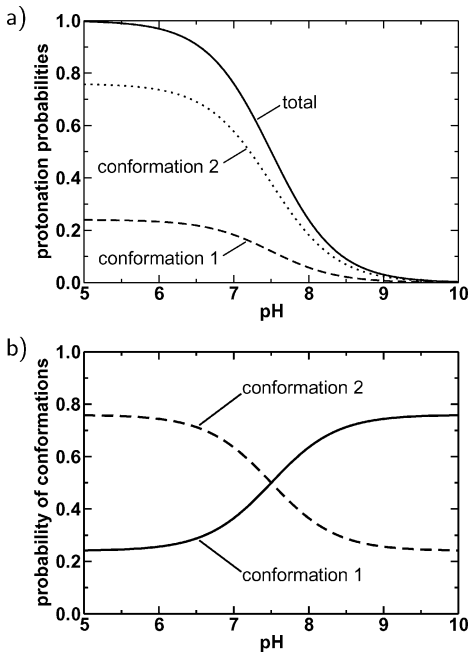

Fig. 2 Titration behavior of a single titratable group in two different conformations. The underlying parameters are $\mathrm{p}K^{\mathrm{intr}}_{\mathrm{a},1} = 7.0$, $\Delta\mathrm{p}K_{\mathrm{a}} = 1.0$, $\Delta G_{\mathrm{conf}} = 0.5$ pK units. (a) Solid line: probability to find the group to be protonated in either of the two conformations; dashed line: probability to find the group to be protonated in conformation 1; dotted line: probability to find the group to be protonated in conformation 2. (b) Probability to find the group in the different conformations, irrespective of its protonation.

The total protonation probability is a sum of the probabilities to find the group protonated in conformation 1 and 2, respectively:

$$\langle x\rangle = \frac{e^{-\beta(\mathrm{pH}-\mathrm{p}K_{a,1})} + e^{-\beta(\Delta G_{conf}+\mathrm{pH}-\mathrm{p}K_{a,1}-\Delta \mathrm{p}K_a)}}{1 + e^{-\beta\Delta G_{conf}} + e^{-\beta(\mathrm{pH}-\mathrm{p}K_{a,1})} + e^{-\beta(\Delta G_{conf}+\mathrm{pH}-\mathrm{p}K_{a,1}-\Delta \mathrm{p}K_a)}}$$
$$= \frac{e^{-\beta \mathrm{pH}}(e^{\beta \mathrm{p}K_{a,1}} + e^{-\beta(\Delta G_{conf}-\mathrm{p}K_{a,1}-\Delta pK_a)})}{1 + e^{-\beta\Delta G_{conf}} + e^{-\beta \mathrm{pH}}(e^{\beta \mathrm{p}K_{a,1}} + e^{-\beta(\Delta G_{conf}-\mathrm{p}K_{a,1}-\Delta pK_a)})}. \quad (18)$$

The titration curve of a molecule with a single titratable group, *i.e.* a monoprotic acid, is always a standard sigmoidal titration curve. Independently of the relative energies and pK_a values of the molecule in its different conformations, the expression for the total protonation probability as a function of pH is equivalent to a sigmoidal Henderson–Hasselbalch curve as given by eqn (2). This statement is valid also for a system with more than two conformations, since eqn (18) can be easily extended to more conformations. From the total titration curve, it is thus impossible to conclude how many different conformations are populated in the protonated or in the deprotonated state. Conformational variability alone can not be the reason for a non-sigmoidal shape of titration curves.

In our titration curves, we monitor the protonation probability as a function of pH. However, it should be kept in mind that experimentally other parameters are monitored such as for instance the chemical shift of a particular group. Such titration curves may differ from a sigmoidal shape if the reporting group has different chemical shifts in different conformations. However, the protonation probability of a monoprotic acid in function of pH has always a standard Henderson–Hasselbalch shape.

Fig. 2(b) shows how the population of the two different conformations changes with pH. The value of $\Delta G_{conf} = G_{conf,2} - G_{conf,1} = 0.5$ pK units for the deprotonated form corresponds to the fact that conformation 1 is at high pH more probable than conformation 2. Variability in the occupation of different conformational states with pH can complicate quantum-chemical computations of pK values since such variability can shift the pK_a value. Thus, these effects need to be considered in the calculation of pK_a values from first principles.

Interaction between two sites can lead to non-sigmoidal titration curves. In contrast to the above example of a single titratable group, titration curves in systems with more than one titratable group can be non-sigmoidal. We consider here a diprotic acid with two distinguishable and strongly interacting titratable sites in a single conformational state. Their intrinsic pK values are 7.0 and 7.1, their interaction energy is 2.0 pK units. As outlined in the Theory section and depicted in Fig. 1(a), such a system can have four different protonation microstates. Their interconversion is characterized by four different microscopic equilibrium constants. Fig. 1(b) displays the changes in the population of the four different microstates with pH. The four microscopic pK values correspond to four pH values at which the different population curves intersect. For example, the $\mathrm{p}K_{10}^{00} = 7.0$ corresponds to the pH at which [00] = [10], *i.e.* the pH at which the two states are equally populated.

Fig. 1(c) illustrates the titration behavior of the system in terms of protonation probabilities. Due to the strong interaction between the two sites, the real-site titration curves have a non-sigmoidal shape. The total protonation probability is a sum of the two quasi-site titration curves, as well as of the two real site titration curves. The quasi-site pK' values of the system are 4.7 and 7.4. Due to the strong coupling between the two groups, the quasi-site pK' values are numerically identical with the macroscopic p$\bar{K}$ values.[18] The two quasi-site pK' values can not be attributed to either of the real sites. As explained for the DSR framework in the Theory section, the two real site titration curves are a linear combination of the two quasi-site titration curves. For the data in Fig. 1, the a_{11} coefficient is 0.56, the other three entries of the a_{ij}-matrix can easily be derived from eqn (11) ($a_{22} = a_{11}$, $a_{12} = a_{21} = 1 - a_{11}$).

Strong interaction is not sufficient to make titration curves non-sigmoidal. A high value for the interaction energy W_{ij} between two groups is necessary but not sufficient to make the titration curves of the individual sites non-sigmoidal. This fact is illustrated in Fig. 3. The two uppermost panels show the sigmoidal titration curves of two non-interacting residues, with intrinsic pK values of 7.0 and 7.1 (see Fig. 3(a.1)), and 5.0 and 9.0 (see Fig. 3(b.1)). If an interaction energy of 1.0 pK units is introduced, the titration curves of the groups with intrinsic pK values of 7.0 and 7.1 get non-sigmoidal (see Fig. 3(a.2)), while those of the groups with intrinsic pK values of 5.0 and 9.0 remain sigmoidal (see Fig. 3(b.2)–(b.5)). To rationalize this divergent behavior, the microscopic pK_r^p values (see Table 1) and corresponding microstate populations (see Fig. 3) need to be considered.

Table 1 Parameters describing the titration behavior of the different types of diprotic acids depicted graphically in Fig. 3. The intrinsic pK values $\mathrm{p}K_1^{intr}$ and $\mathrm{p}K_2^{intr}$ and the interaction energy W_{12} are the quantities that enter into the calculation of protonation microstate energies by eqn (15). The meaning of the ion type labels are explained in the legend of Fig. 3. The microscopic $\mathrm{p}K_r^p$ values and macroscopic p$\bar{K}$ values are calculated from the protonation microstate energies *via* eqn (7) and eqn (8), respectively. DSR parameters are derived as described in the Theory section

					Microscopic				Macroscopic		DSR			
$\mathrm{p}K_1^{intr}$	$\mathrm{p}K_2^{intr}$	W_{12}	Ionic nature	Reference state	$\mathrm{p}K_{11}^{01}$	$\mathrm{p}K_{11}^{10}$	$\mathrm{p}K_{01}^{00}$	$\mathrm{p}K_{10}^{00}$	$\mathrm{p}\bar{K}_1$	$\mathrm{p}\bar{K}_2$	$\mathrm{p}K'_1$	$\mathrm{p}K'_2$	a_{11}	Panel in Fig. 3
7.0	7.1	1.0	AA	11	7.0	7.1	8.1	8.0	6.7	8.4	6.8	8.3	0.56	a.2
			AC	10	6.0	7.1	8.1	7.0	6.0	8.1	6.0	8.1	0.93	a.3
			CA	01	7.0	6.1	7.1	8.0	6.0	8.1	6.1	8.0	0.11	a.4
			CC	00	6.0	6.1	7.1	7.0	5.7	7.4	5.8	7.3	0.56	a.5
5.0	9.0	1.0	AA	11	5.0	9.0	10.0	6.0	5.0	10.0	5.0	10.0	0.99	b.2
			AC	10	4.0	9.0	10.0	5.0	4.0	10.0	4.0	10.0	0.99	b.3
			CA	01	5.0	8.0	9.0	6.0	5.0	9.0	5.0	9.0	0.99	b.4
			CC	00	4.0	8.0	9.0	5.0	4.0	9.0	4.0	9.0	0.99	b.5

 This journal is © The Royal Society of Chemistry and Owner Societies 2006

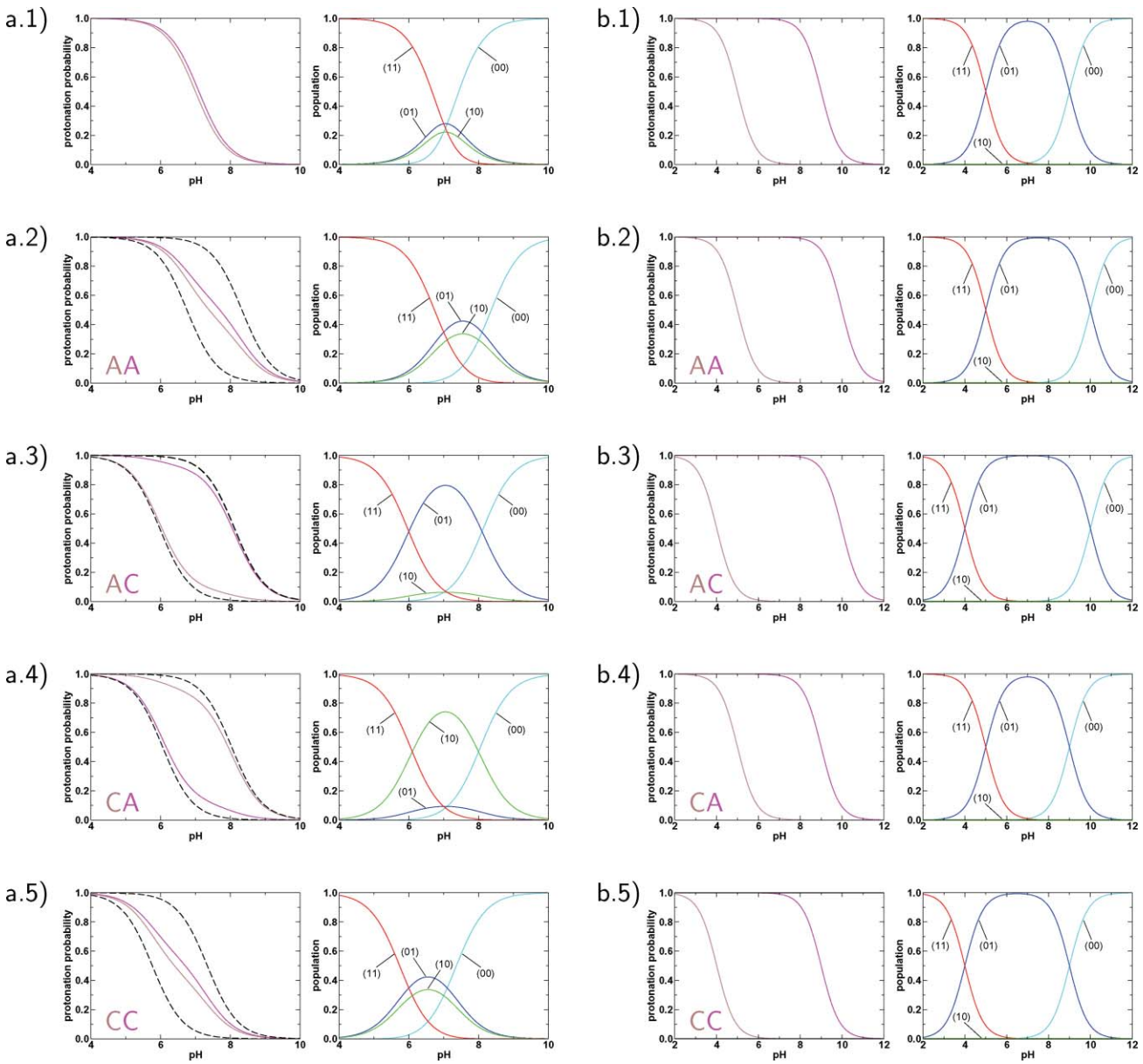

Fig. 3 Effect of the interaction energy, the difference in the intrinsic pK values, and the ionic nature of two titratable groups on their titration behavior. Labels in the lower four rows of panels denote the anionic (A) or cationic (C) nature of the two groups. Anionic groups have a negatively charged deprotonated form and a neutral protonated form. Cationic groups have a positively charged protonated form and a neutral deprotonated form. The protonation probabilities of site 1 (lower intrinsic pK value) and site 2 (higher intrinsic pK value), and the probabilities of the different microstates are color-coded as in Fig. 1. (a.1) and (b.1): Titration behavior of two non-interacting groups. Intrinsic and quasi-site pK' values coincide (7.0 and 7.1 in panel (a.1), 5.0 and 9.0 in panel (b.1)). (a.2)–(a.4): Titration behavior of two interacting groups with the same intrinsic pK values as in panel (a.1). Sigmoidal quasi-site titration curves are given as dashed lines for comparison. Corresponding parameters are given as first block of data in Table 1. (b.2)–(b.4): Titration behavior of two interacting groups with the same intrinsic pK values as in panel (b.1). Sigmoidal quasi-site titration curves coincide with the real site titration curves. Corresponding parameters are given as second block of data in Table 1.

For Fig. 3(b.2), pK_{11}^{01} is considerably smaller than pK_{11}^{10}. The (10) microstate is therefore never populated. Consequently, site 2 is protonated in the pH range where site 1 titrates. In contrast, site 1 is deprotonated in the pH range where site 2 titrates. Since the interaction energy corresponds to the difference in the pK value of site 1 depending on whether site 2 is protonated or deprotonated and *vice versa*, it does not have any effect on the shape of the individual titration curves. For Fig. 3(a.2), pK_{11}^{01} and pK_{11}^{10} are similar, and the two singly protonated microstates have a similar probability. In this case, site 1 may occur to be protonated or deprotonated at almost equal probability in the pH-range where site 2 titrates and *vice versa.* Consequently, the interaction between the two sites does in this case modify the shape of the individual titration curves.

The microstate probabilities and microscopic pK_r^p values are the relevant quantities to decide whether a high interaction energy between two groups leads to non-sigmoidal titration behavior. While the treatment of cationic and anionic titratable groups is

a)

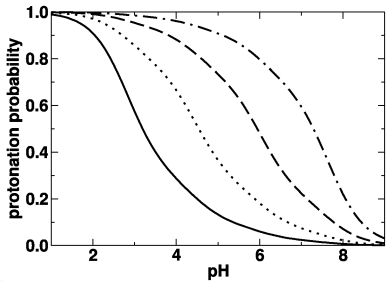

$$\mathrm{p}K_i' = \begin{pmatrix} 2.8 \\ 4.5 \\ 6.0 \\ 7.7 \end{pmatrix} \quad \{a_{ij}\} = \begin{pmatrix} 0.70 & 0.21 & 0.07 & 0.02 \\ 0.21 & 0.52 & 0.20 & 0.07 \\ 0.07 & 0.20 & 0.52 & 0.21 \\ 0.02 & 0.07 & 0.21 & 0.70 \end{pmatrix}$$

b)

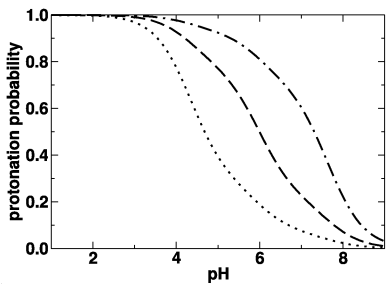

$$\mathrm{p}K_i' = \begin{pmatrix} 4.3 \\ 6.0 \\ 7.6 \end{pmatrix} \quad \{a_{ij}\} = \begin{pmatrix} 0.72 & 0.22 & 0.06 \\ 0.22 & 0.56 & 0.22 \\ 0.06 & 0.22 & 0.72 \end{pmatrix}$$

c)

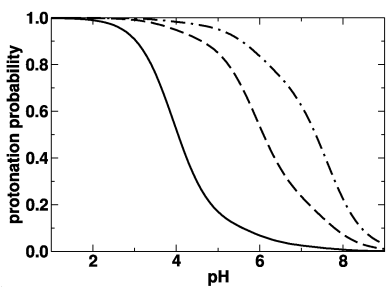

$$\mathrm{p}K_i' = \begin{pmatrix} 3.9 \\ 5.9 \\ 7.6 \end{pmatrix} \quad \{a_{ij}\} = \begin{pmatrix} 0.89 & 0.09 & 0.02 \\ 0.08 & 0.69 & 0.23 \\ 0.03 & 0.22 & 0.75 \end{pmatrix}$$

d)

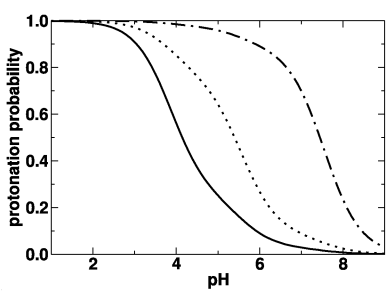

$$\mathrm{p}K_i' = \begin{pmatrix} 3.9 \\ 5.6 \\ 7.5 \end{pmatrix} \quad \{a_{ij}\} = \begin{pmatrix} 0.75 & 0.22 & 0.03 \\ 0.23 & 0.69 & 0.08 \\ 0.02 & 0.09 & 0.89 \end{pmatrix}$$

e)

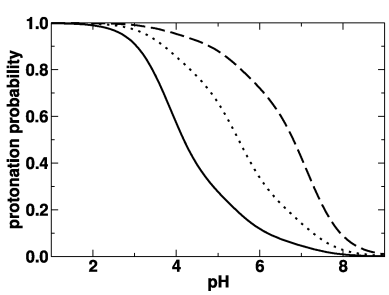

$$\mathrm{p}K_i' = \begin{pmatrix} 3.8 \\ 5.5 \\ 7.1 \end{pmatrix} \quad \{a_{ij}\} = \begin{pmatrix} 0.72 & 0.22 & 0.06 \\ 0.22 & 0.56 & 0.22 \\ 0.06 & 0.22 & 0.72 \end{pmatrix}$$

Fig. 4 Titration behavior of four interacting residues in a wild-type and four mutant scenarios. The real site titration behavior of the four different titratable sites is presented graphically (solid line: site 1, $\mathrm{p}K_{\mathrm{a},1}^{\mathrm{intr}} = 6.0$; dotted line: site 2, $\mathrm{p}K_{\mathrm{a},2}^{\mathrm{intr}} = 6.5$; dashed line: site 3, $\mathrm{p}K_{\mathrm{a},3}^{\mathrm{intr}} = 7.0$; dashed-dotted line: site 4, $\mathrm{p}K_{\mathrm{a},4}^{\mathrm{intr}} = 7.5$). All pairwise interaction energies are set to 1.0 pK unit. The corresponding DSR parameters are given. (a) Wildtype scenario, all four residues are titratable. (b)–(e) Residues 1–4, respectively, have been changed to a neutral non-titratable residue. The effect of the mutations on the remaining three titratable residues becomes obvious from comparison with (a).

 This journal is © The Royal Society of Chemistry and Owner Societies 2006

identical in the calculation of protonation microstate energies (see eqn (15)) and all subsequent analyses, the relationship between the microscopic and intrinsic pK values is modulated by the different definition of the reference form for cationic and anionic groups. Due to the definition of the reference form to be uncharged, it corresponds to different protonation forms of anionic and cationic groups (see Table 1). If the two interacting groups are both anionic or both cationic (see Fig. 3(a.2) and (a.5)), the intrinsic pK values correspond to the microscopic pK_{11}^{01} and pK_{11}^{10} values (two anionic sites), and pK_{01}^{00} and pK_{10}^{00} values (two cationic sites, see Table 1). In these two cases, the similarity of the intrinsic pK values results in a set of microscopic pK_r^p values that leads to a similar population of the (01) and (10) microstates, and thus to an effect of the interaction energy on the shape of the titration curves. However, if the two interacting groups have different ionic nature (see Fig. 3(a.3) and (a.4)), the intrinsic pK values correspond to microscopic pK values that belong to different macroscopic protonation equilibria. For example, if the first site is anionic and the second site is cationic (see Fig. 3(a.3)), the intrinsic pK values correspond to the microscopic pK_{11}^{10} and pK_{10}^{00} values (see Table 1), which are involved in the release of the first and second proton, respectively. In this case, a high interaction energy shifts the individual titration curves, but only weakly affects their shape.

The effect of mutations on the behavior of interacting titratable residues

In order to demonstrate how mutations of titratable residues change the behavior of other interacting titratable residues, we have investigated the titration behavior of a cluster of four interacting residues. The four residues have intrinsic pK values of 6.0, 6.5, 7.0 and 7.5. All of them are cationic residues and interact with a pairwise interaction energy of 1.0 pK unit. Analyzing Fig. 4, it can be seen that the pK' values are similar, however not identical to the pH at the midpoint of the titration curves. Thus, the midpoint of the titration curves gives a first guess of a thermodynamically clearly defined pK_a value, which can then be refined by a more rigorous fitting.

As can be read from Fig. 4, mutations of one of the titratable residues to a neutral, non-titratable residue considerably change the titration behavior of the remaining three residues. For example, the mutation of site 2 (see Fig. 4(c)), site 3 (see Fig. 4(d)) or site 4 (see Fig. 4(e)) shifts the titration curve of site 1 to higher pH values compared to the wild-type scenario (see Fig. 4(a)). This effect is reflected by the change of approximately 1 pK unit in the lowest quasi-site pK' value from Fig. 4(a) to (c), (d) and (e). On the other hand, mutation of sites 1, 2 or 3 (see Fig. 4(b), (c) and (d), respectively) does not considerably change the titration curve of site 4. From this simple example of four interacting residues, it is thus obvious that mutational changes of titratable residues can lead to changes in the behavior of other titratable residues. These changes are not trivial to predict but need to be considered in the interpretation of experimental results. Experimental mutational studies directed for example at the functional role of a certain titratable residue should therefore always be accompanied by a thorough analysis of the effect of the mutation on other titratable residues.

Conclusions

Most proteins contain multiple titratable residues that interact electrostatically. Interaction between titratable sites can lead to irregular, non-sigmoidal titration curves of the individual sites. Such non-sigmoidal titration curves cannot be described by a single thermodynamically precisely-defined pK value. As demonstrated in the present paper, macroscopic $p\bar{K}$ values, microscopic pK_r^p values, and the quasi-site pK' values of the decoupled sites representation have however a clear connection to the thermodynamics of the system and can adequately characterize the titration behavior of proteins. Titration curves become irregular only if two sites have a high pairwise interaction energy, and if their microscopic pK_r^p values are similar. Conformational variability alone does not lead to an irregular shape of titration curves. Nevertheless, conformational flexibility can shift pK values and should therefore be considered carefully in any approach to calculate pK_a values using quantum-chemical methods.

If a mutation of a titratable residue is introduced in a protein, it can severely affect the titration behavior of other interacting titratable sites. Changes in the macroscopic titration behavior can thus not be attributed simply to a lack of the contribution of the mutated titratable residue. The interaction among titratable residues complicates the analysis of mutational studies directed at identifying a functional role for a certain titratable residue. To obtain conclusive results, the mutational studies should be accompanied by an analysis of the microscopic titration behavior of the other titrating residues in the wild-type and the mutant system.

Acknowledgements

This work was supported by the Deutsche Forschungsgemeinschaft (Forschergruppe 490 DFG UL 174/4-3, and DFG UL 174/6-2). A. R. K. thanks the Boehringer Ingelheim Fonds for a doctoral fellowship.

References

1 N. Calimet and G. M. Ullmann, The effect of a transmembrane pH gradient on protonation probabilities of bacteriorhodopsin, *J. Mol. Biol.*, 2004, **339**, 571–589.
2 A. R. Klingen and G. M. Ullmann, Negatively charged residues and hydrogen bonds tune the ligand histidine pK_a values of Rieske iron–sulfur proteins, *Biochemistry*, 2004, **43**, 12383–12389.
3 A. Taly, P. Sebban, J. C. Smith and G. M. Ullmann, The position of Q_B in the photosynthetic reaction center depends on pH: a theoretical analysis of the proton uptake upon Q_B reduction, *Biophys. J.*, 2003, **84**, 2090–2098.
4 Y. Song, J. Mao and M. R. Gunner, Calculation of proton transfers in bacteriorhodopsin bR and M intermediates, *Biochemistry*, 2003, **42**, 9875–9888.
5 R. E. Georgescu, E. G. Alexov and M. R. Gunner, Combining conformational flexibility and continuum electrostatics for calculating pK_as in proteins, *Biophys. J.*, 2002, **83**, 1731–1748.
6 B. Rabenstein and E. W. Knapp, Calculated pH-dependent population of carbon-monoxy-myoglobin conformers, *Biophys. J.*, 2001, **80**, 1141–1150.
7 B. Rabenstein, G. M. Ullmann and E.-W. Knapp, Energetics of electron transfer and protonation reactions of the quinones in the photosynthetic reaction center of *Rhodopseudomonas viridis*, *Biochemistry*, 1998, **37**, 2488–2495.
8 B. Rabenstein, G. M. Ullmann and E.-W. Knapp, Calculation of protonation patterns in proteins with conformational relaxation-application

to the photosynthetic reaction center, *Eur. Biophys. J.*, 1998, **27**, 628–637.
9 E. Demchuk and R. C. Wade, Improving the Continuum Dielectric Approach to Calculating pK_as of Ionizable Groups in Proteins, *J. Phys. Chem.*, 1996, **100**, 17373–17387.
10 P. Beroza and D. A. Case, Including Side Chain Flexibility in Continuum Electrostatic Calculations of Protein Titration, *J. Phys. Chem.*, 1996, **100**, 20156–20163.
11 M. K. Gilson, Multiple-Site Titration and Molecular Modelling: Two Rapid Methods for Computing Energies and Forces for Ionizable Groups in Proteins, *Proteins: Struct., Funct., Genet.*, 1993, **15**, 266–282.
12 A. Onufriev, A. Smondyrev and D. Bashford, Proton affinity changes driving unidirectional proton transport in the bacteriorhodopsin photocycle, *J. Mol. Biol.*, 2003, **332**, 1183–1193.
13 B. Rabenstein and E. W. Knapp, Calculated pH-dependent population and protonation of carbon-monoxy-myoglobin conformers, *Biophys. J.*, 2001, **80**, 1141–1150.
14 T. You and D. Bashford, Conformation and Hydrogen Ion Titration of Proteins: A Continuum Electrostatic Model with Conformational Flexibility, *Biophys. J.*, 1995, **69**, 1721–1733.
15 M. Felemez, P. Bernard, G. Schlewer and B. Spiess, Inframolecular Protonation Process of myo-Inositol 1,4,5-Tris(phosphate) and Related Compounds: Dynamics of the Intramolecular Interactions and Evidence of C–HO Hydrogen Bonding, *J. Am. Chem. Soc.*, 2000, **122**, 3156–3165.
16 E. Bombarda, N. Morellet, H. Cherradi, B. Spiess, S. Bouaziz, E. Grell, B. P. Roques and Y. Mely, Determination of the pK_a of the four Zn^{2+}-coordinating residues of the distal finger motif of the HIV^{-1} nucleocapsid protein: consequences on the binding of Zn^{2+}, *J. Mol. Biol.*, 2001, **310**, 659–672.
17 A. Onufriev, D. A. Case and G. M. Ullmann, A novel view of pH titration in biomolecules, *Biochemistry*, 2001, **40**, 3413–3419.
18 G. M. Ullmann, Relations between protonation constants and titration curves in polyprotic acids: A critical view, *J. Phys. Chem. B*, 2003, **107**, 1263–1271.
19 A. Onufriev and G. M. Ullmann, Decomposing complex ligand binding into simple components: connections between microscopic and macroscopic models, *J. Phys. Chem. B*, 2004, **108**, 11157–11169.
20 A. Warshel and S. T. Russel, Calculations of Electrostatic Interaction in Biological Systems and in Solution, *Q. Rev. Biophys.*, 1984, **17**, 283–422.
21 C. Tanford and J. G. Kirkwood, Theory of Protein Titration Curves, *J. Am. Chem. Soc.*, 1957, **79**, 5333–5347.
22 C. Tanford and R. Roxby, Interpretation of Protein Titration Curves. Application to Lysozyme, *Biochemistry*, 1972, **11**, 2192–2198.
23 D. Bashford and M. Karplus, Multiple-Site Titration Curves of Proteins: An Analysis of Exact and Approximate Methods for Their Calculations, *J. Phys. Chem.*, 1991, **95**, 9556–9561.
24 J. L. Sudmeier and C. N. Reilley, Nuclear Magnetic Resonance Studies of Protonation of Polyamine and Aminocarboxylate Compounds in Aqueous Solution, *Anal. Chem.*, 1964, **36**, 1698–1706.
25 M. Borkovec and G. J. M. Koper, Ising Models of Polyprotic Acids and Bases, *J. Phys. Chem.*, 1994, **98**, 6038–6045.
26 J. A. Schellman, Macromolecular Binding, *Biopolymers*, 1975, **14**, 999–1018.
27 B. Noszal, Group Constant: A measure of Submolecular Basicity, *J. Phys. Chem.*, 1986, **90**, 4104–4110.
28 I. M. Klotz, *Ligand-Receptor Energetics*, Wiley & Sons Inc., New York, 1997.
29 J. Wyman and S. J. Gill, *Binding and Linkage*, University Science Books, Mill Valley, CA, 1990.
30 D. Bashford and M. Karplus, pK_as of ionizable groups in proteins: atomic detail from a continuum electrostatic model, *Biochemistry*, 1990, **29**, 10219–10225.
31 G. M. Ullmann and E.-W. Knapp, Electrostatic models for computing protonation and redox equilibria in proteins, *Eur. Biophys. J.*, 1999, **28**, 533–551.
32 W. Press, S. Teukolsky, W. Vetterling and B. Flannery, *Numerical Recipes in C,*Cambridge University Press, Cambridge UK, 2nd edn, 1992.

 This journal is © The Royal Society of Chemistry and Owner Societies 2006